

ARTICLE



Oncogenic RAS promotes leukemic transformation of CUX1-deficient cells

Ningfei An^{1,2}, Saira Khan^{1,2}, Molly K. Imgruet^{1,3}, Lia Jueng^{1,2}, Sandeep Gurbuxani¹ and Megan E. McNerney^{1,2,3}

© The Author(s), under exclusive licence to Springer Nature Limited 2023

-7/del(7q) is prevalent across subtypes of myeloid neoplasms. *CUX1*, located on 7q22, encodes a homeodomain-containing transcription factor, and, like -7/del(7q), *CUX1* inactivating mutations independently carry a poor prognosis. As with loss of 7q, *CUX1* mutations often occur early in disease pathogenesis. We reported that *CUX1* deficiency causes myelodysplastic syndrome in mice but was insufficient to drive acute myeloid leukemia (AML). Given the known association between -7/del(7q) and RAS pathway mutations, we mined cancer genome databases and explicitly linked *CUX1* mutations with oncogenic RAS mutations. To determine if activated RAS and *CUX1* deficiency promote leukemogenesis, we generated mice bearing *Nras*^{G12D} and *CUX1*-knockdown which developed AML, not seen in mice with either mutation alone. Oncogenic RAS imparts increased self-renewal on *CUX1*-deficient hematopoietic stem/progenitor cells (HSPCs). Reciprocally, *CUX1* knockdown amplifies RAS signaling through reduction of negative regulators of RAS/PI3K signaling. Double mutant HSPCs were responsive to PI3K or MEK inhibition. Similarly, low expression of *CUX1* in primary AML samples correlates with sensitivity to the same inhibitors, suggesting a potential therapy for malignancies with *CUX1* inactivation. This work demonstrates an unexpected convergence of an oncogene and tumor suppressor gene on the same pathway.

Oncogene; <https://doi.org/10.1038/s41388-023-02612-x>

INTRODUCTION

Deletion of part or all of chromosome 7 [-7/del(7q)] is a recurrent, adverse-risk cytogenetic change in pediatric and adult myeloid malignancies [1]. Deletions of chromosome 7 occur in clonal hematopoiesis and can be an initiating event in myeloid transformation [2–5]. We reported that the non-clustered HOX-family transcription factor, *CUX1*, is a haploinsufficient tumor-suppressor gene encoded on 7q22 [6]. *CUX1* loss-of-function mutations are recurrent in myeloid malignancies and are an independent prognostic indicator of poor outcome [7–9]. Mutations in *CUX1* include nonsense truncating mutations, deleterious missense mutations in conserved protein domains, and mutations predicted to alter *CUX1* splicing [1]. *CUX1* mutations are found in clonal hematopoiesis and occur early in myeloid transformation, suggesting *CUX1* is a gatekeeper in myeloid neoplasia [7, 10–12]. Overall, patient data assert the clinical similarities between loss of 7q and *CUX1* mutations.

CUX1 is highly conserved across species, ubiquitous, and essential for embryogenesis [13–15]. *CUX1* has critical roles in the development of several different tissues including hematopoietic [16–19]. The human *CUX1* protein is 1505 amino acids and harbors a homeodomain and three CUT-repeat DNA binding domains. We reported that *CUX1* binds widely across the genome with a preference for active, distal enhancers [20]. In line with these diverse functions, *CUX1* regulates several distinct transcriptional pathways [21]. In hematopoietic cells, *CUX1* haploinsufficiency is repeatedly associated with gene signatures of increased

proliferation [6, 19, 20, 22]. We reported that *CUX1*-knockdown in mice leads to myelodysplastic syndrome (MDS) and myeloproliferative neoplasms (MPNs), indicating that loss of this single 7q gene is sufficient to cause disease [19, 22]. However, loss of *CUX1* is not sufficient to cause overt acute myeloid leukemia (AML), raising the question of whether additional genetic events cooperate in leukemogenesis.

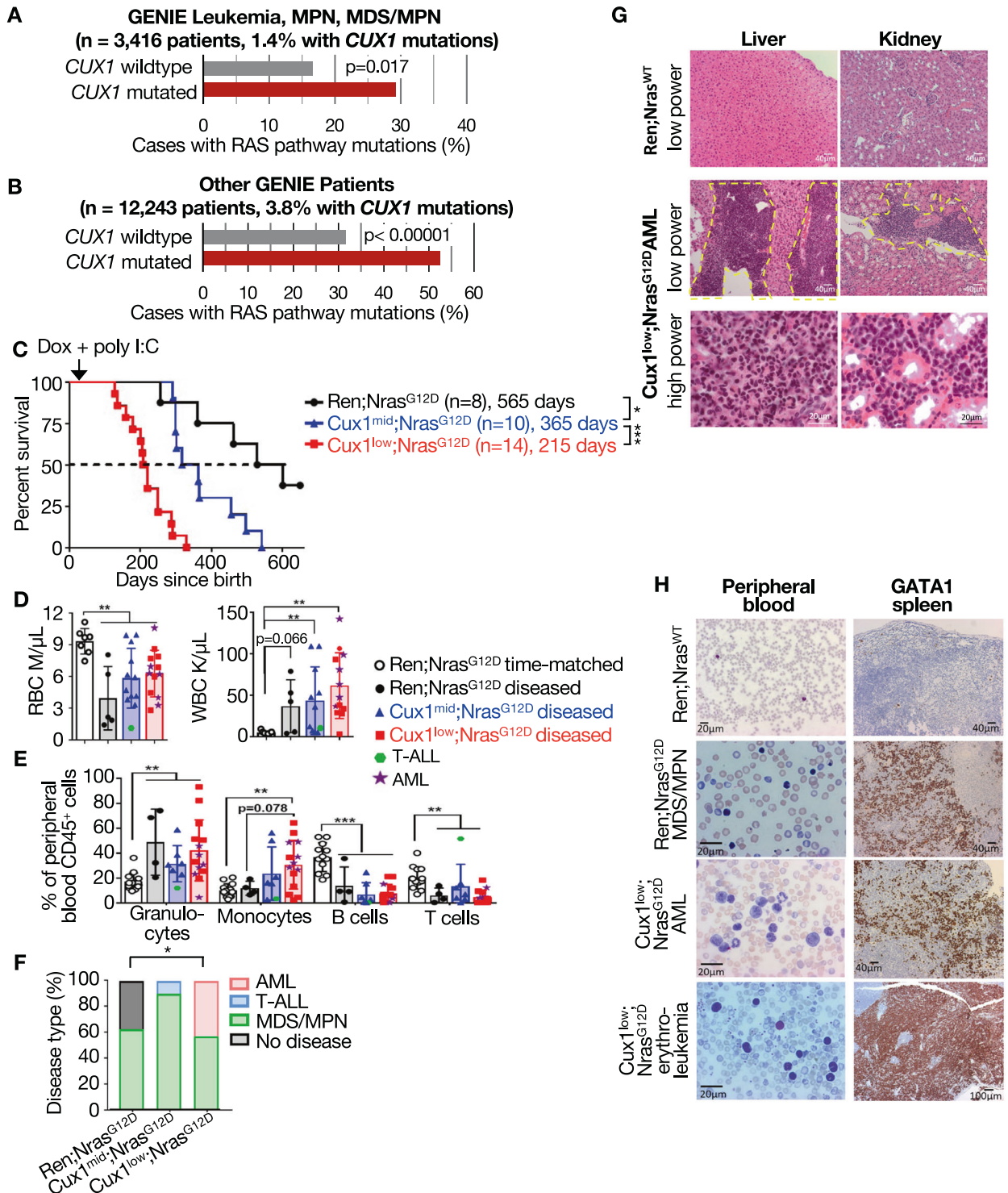
Monosomy 7 has long been associated with gain-of-function mutations in the RAS pathway. This co-occurrence is observed in myeloid malignancies arising *de novo*, after chemotherapy, or in inherited predisposition syndromes [23, 24]. Juvenile myelomonocytic leukemia (JMML) provides a striking example of this; the majority of cases harbor a RAS pathway mutation with -7/del(7q) being the single most common co-occurring cytogenetic abnormality [25, 26]. We reported that oncogenic RAS pathway mutations in -7/del(7q) myeloid malignancies are enriched in cases with deletions spanning *CUX1* [27]. This co-occurrence suggests positive genetic epistasis between gain of RAS signaling and loss of *CUX1* and, on the surface, aligns with the paradigm of collaboration between Class I signaling mutations and Class II mutations in transcriptional regulators [28].

RAS pathway alterations observed in *CUX1*-deleted myeloid malignancies include gain-of-function mutations of *NRAS*, *KRAS*, *PTPN11*, and *RIT1*, and deletion or loss-of-function mutations of *NF1* and *CBL* [27]. Intriguingly, inherited mutations in these same genes occur in RASopathy syndromes which carry a risk of myeloid transformation, particularly with monosomy 7 [29]. RASopathy

¹Department of Pathology, The University of Chicago, Chicago, IL, USA. ²Department of Pediatrics, Hematology/Oncology, The University of Chicago, Chicago, IL, USA. ³The University of Chicago Medicine Comprehensive Cancer Center, The University of Chicago, Chicago, IL, USA. ✉email: megan.mcnerney@uchospitals.edu

Received: 16 September 2022 Revised: 23 January 2023 Accepted: 25 January 2023

Published online: 01 February 2023



mutations promote growth factor receptor-independent activation of downstream signaling effectors, such as RAF-MEK-ERK and PI3K, culminating in enhanced proliferation and cell survival. Among these genes, *NRAS* is the most frequently somatically mutated in myeloid cancers [30]. Mice expressing oncogenic *Nras*^{G12D} develop indolent myeloid disorders and not AML [31].

Here we report the significant and wide-spread co-occurrence of RAS pathway and *CUX1* mutations across cancer types. *CUX1*-knockdown mice harboring *Nras*^{G12D} develop AML with high-penetrance, constituting a genetically accurate in vivo model of

high-risk AML. Our mechanistic studies indicate that *Cux1* deficiency and oncogenic RAS unexpectedly converge to amplify RAS signaling to drive tumorigenesis.

RESULTS

CUX1 and RAS driver mutations co-occur in myeloid malignancies and solid tumors

We previously observed that the most frequently mutated genes in -7/del(7q) myeloid malignancies were driver mutations in the

Fig. 1 **CUX1 and RAS driver mutations co-occur across tumor types and cooperate in myeloid leukemogenesis.** Samples from the indicated tumor types were divided into those with and without *CUX1* mutations. The frequency of RAS pathway driver mutations within *CUX1* wildtype and mutated subsets is shown. Driver mutations were annotated by cBioPortal as hotspots, an OncoKB driver [63], or present in ≥ 5 cases in cBioPortal or COSMIC databases. **A** Leukemia, MPN, and MDS/MPN patients from GENIE Cohort v.12.1 were queried via cBioPortal for driver mutations in *CUX1* and RAS pathway genes (*KRAS*, *HRAS*, *NRAS*, *CBL*, and *PTNP11*). *NFI*, *RIT1*, and *SOS1* were excluded from this analysis due to insufficient profiling for these genes. **B** The entire remaining GENIE cohort was assessed for driver mutations in *CUX1* and RAS pathway genes (*KRAS*, *HRAS*, *NRAS*, *CBL*, *PTNP11*, *NFI*, *RIT1*, and *SOS1*). In instances with multiple samples from the same patient, only patient-level data were analyzed. **C** 4–6 week-old mice were treated with doxycycline and poly I:C as described in the Methods. Kaplan-Meier survival plot of indicated mice after treatment is shown. Significance was determined by log-rank test. The median survival post-birth is shown. **D** Peripheral red blood red (RBC) and white blood cell (WBC) counts are shown. Ren;Nras^{G12D} mice that had been treated for the same length of time (Ren;Nras^{G12D} time-matched) are included for comparison to diseased Cux1^{mid}; Nras^{G12D} and Cux1^{low}; Nras^{G12D}. Data from mice diagnosed with T-cell acute lymphoblastic leukemia (T-ALL, $n = 1$) or AML ($n = 6$) are indicated by green hexagons or purple stars, respectively. **E** Flow cytometry was performed for leukocyte subsets: granulocytes (CD11b⁺/Gr1⁺), monocytes (CD11b⁺/Gr1⁻), B cells (B220⁺), and T cells (CD3⁺). **F** The distribution of disease phenotypes observed classified based on the Bethesda criteria [34] in the indicated genotypes is shown. A significant increase in myeloid disease and AML was observed in Cux1^{low};Nras^{G12D} mice compared to Ren;Nras^{G12D} ($p = 0.0364$ and $p = 0.051$, respectively, Fisher's exact test). **G** H&E staining indicates Cux1^{low};Nras^{G12D} mice with AML have organ infiltration with myeloid cells. Infiltrates are encircled in yellow dashed lines, and higher magnification images show the leukemic cells. **H** Representative images of Wright-Giemsa stained peripheral blood are shown. Immunohistochemistry for GATA1 in the spleen is shown. For **A**, **B**, **D**, and **E**, two-tailed Student *t* test was used to assess statistical significance. * $p < 0.05$, ** $p < 0.01$, and *** $p < 0.001$.

RAS pathway [27]. To determine if *CUX1* inactivation is directly linked to RAS pathway mutations, we mined the AACR Project GENIE database: <https://www.aacr.org/professionals/research/aacr-project-genie>. Among 3416 myeloid malignancy patients, 1.4% harbored *CUX1* inactivating mutations. Compared to *CUX1* wild-type patients, *CUX1* mutated cases had a significantly higher frequency of driver mutations in *NRAS*, *KRAS*, *HRAS*, *PTNP11*, or *CBL* (Fig. 1A and Supplementary Fig. 1A). This suggests that the association of monosomy 7 and RAS mutations is partly due to a genetic interaction specifically between *CUX1* and RAS.

CUX1 mutations are also recurrent across solid tumors [9]. We thus enquired if the association between RAS and *CUX1* holds true in non-myeloid malignancies. We assessed all available non-myeloid malignancy patients in the GENIE database profiled for *CUX1* and RAS pathway genes. While RAS driver mutations were present in 31.6% of *CUX1* wildtype tumors, 52.5% of *CUX1* mutated counterparts harbored oncogenic RAS mutations (Fig. 1B). We corroborated this finding with TCGA datasets across a variety of solid tumor types (Supplementary Fig. 1B). These findings indicate that the genetic interaction between *CUX1* loss and gain-of-function of RAS is a universal feature of tumorigenesis.

The combination of Nras^{G12D} and CUX1-knockdown drives myeloid leukemia transformation

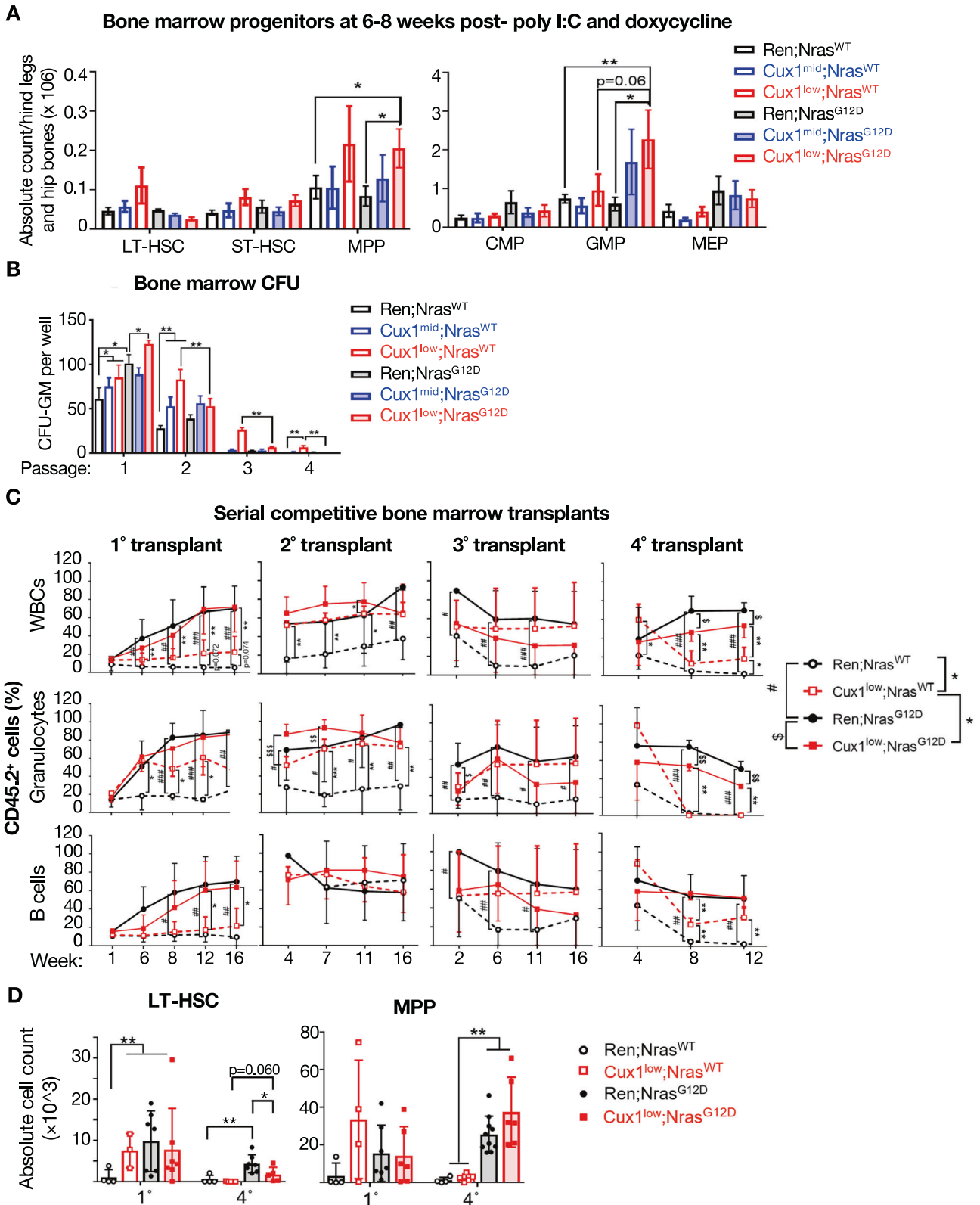
To test the impact of combinatorial *CUX1* deficiency and oncogenic RAS, we crossed our inducible, shRNA-based *CUX1*-knockdown mouse lines, Cux1^{mid} and Cux1^{low} [19], with Mx1-Cre;LSL-Nras^{G12D} mice expressing Nras^{G12D} from the endogenous locus [32]. Cux1^{mid} has 58% and Cux1^{low} has 42% residual *CUX1* mRNA in Lin⁻/Sca1⁺/Kit⁺ (LSK) cells [19]. As most patients retain one wildtype allele of *CUX1*, *CUX1*-knockdown mice approximate the haploinsufficient levels present in patient samples with $-7/\text{del}(7q)$ or *CUX1* mutations [6, 9, 33]. Our breeding scheme generated Cux1^{mid};Nras^{G12D} (Cux1^{mid};⁻;M2rtTA^{+/+};Mx1-Cre^{+/+};Nras^{G12D};⁻), Cux1^{low};Nras^{G12D} (Cux1^{low};⁻;M2rtTA^{+/+};Mx1-Cre^{+/+};Nras^{G12D};⁻) and Ren;Nras^{G12D} littermate controls (Ren.713^{+/+};M2rtTA^{+/+};Mx1-Cre^{+/+};Nras^{G12D};⁻). We activated shRNA and Nras^{G12D} expression with doxycycline and poly I:C at 4–6 weeks of age. Consistent with prior reports, Ren;Nras^{G12D} mice developed late-onset disease with incomplete penetrance [31] (Fig. 1C). In contrast, Cux1^{mid};Nras^{G12D} mice had earlier mortality ($p = 0.0123$) affecting 100% of mice, which was also faster than Cux1^{mid};Nras^{WT} ($p = 0.0003$, Supplementary Fig. 2). Among the experimental groups, Cux1^{low};Nras^{G12D} mice had the shortest survival time, with complete disease penetrance (Fig. 1C and supplementary Fig. 2). When diseased, Ren;Nras^{G12D}, Cux1^{mid};Nras^{G12D}, and Cux1^{low};Nras^{G12D} developed similar levels of anemia

and leukocytosis comprised of increased myeloid cells at the expense of lymphoid cells (Fig. 1D and E). For comparison, we included Ren;Nras^{G12D} mice that had been treated for the same length of time (Ren;Nras^{G12D} time-matched). For most metrics, Cux1^{mid};Nras^{G12D} and Cux1^{low};Nras^{G12D} mice were significantly different from Ren;Nras^{G12D} treated for the same time length (Fig. 1D and E). Thus, some hematopoietic indices are eventually comparable across the three experimental groups at the time of disease, however, *CUX1*-knockdown accelerates the onset and penetrance of these changes.

Following the Bethesda criteria [34], all diseased mice developed hematopoietic malignancies which were most often MDS/MPN, similar to JMML in pediatric patients or chronic myelomonocytic leukemia (CMML) in adults. Whereas 5/8 (62.5%) of Ren;Nras^{G12D} mice developed MDS/MPN, consistent with previous reports [31], 9/10 (90%) of Cux1^{mid};Nras^{G12D} counterparts acquired MDS/MPN (Fig. 1F). In stark contrast, only Cux1^{low};Nras^{G12D} mice developed AML, occurring in 6/14 (42.9%). AMLs were characterized by increased circulating blasts and organ infiltration (Fig. 1G and H). While most of the AMLs in Cux1^{low};Nras^{G12D} were morphologically myeloblastic or monocytic, one mouse developed in erythroleukemia characterized by pervasive GATA1⁺ erythroblasts in the spleen (Fig. 1H). These data demonstrate that the combination of *CUX1*-knockdown with Nras^{G12D} uniquely drives leukemic transformation, not seen with either mutation alone.

Nras^{G12D} confers increased self-renewal properties on Cux1^{low} hematopoietic stem and progenitor cells

We reported that *CUX1*-knockdown promotes the expansion of progenitor and mature myeloid cells, but phenotypic long-term hematopoietic stem cells (LT-HSC) are eventually depleted and exhaust [19]. That *Cux1* deficiency leads to HSC exhaustion is incongruent with transformation and suggests that a second genetic alteration is required for the long-term self-renewal of *CUX1*-deficient leukemic stem cells. As gain-of-function mutations in the RAS pathway increase HSC and multipotent progenitor (MPP) self-renewal [35, 36], we hypothesized that Nras^{G12D} confers self-renewal properties on *CUX1*-knockdown hematopoietic stem and progenitor cells (HSPC). To test this, we first assessed the combinatorial impact of *CUX1*-knockdown and Nras^{G12D} on HSPC population frequencies at the pre-disease stage, 6–8 weeks after transgene induction. Compared to Nras^{G12D} alone, Cux1^{low};Nras^{G12D} mice had an expansion in MPPs and granulocyte-monocyte progenitors (GMP) at this early time point (Fig. 2A). Consistent with a phenotypic expansion of progenitor populations, Cux1^{low};Nras^{G12D} bone marrow had the highest frequency of



granulocyte/monocyte colony forming units (CFU-GM, Fig. 2B, passage 1). CUX1-knockdown; $Nras^{G12D}$ cells did not have substantially increased CFU serial-replating capacity (Fig. 2B). On the other hand, $Nras^{G12D}$ cells alone also do not have increased self-renewal in this in vitro assay (Fig. 2B) [37]. These data indicate that

the combination of CUX1-knockdown and $Nras^{G12D}$ leads to an expanded myeloid progenitor population.

To test self-renewal capacity more rigorously, we performed serial, competitive bone marrow transplantation assays. CD45.2⁺ experimental bone marrow was mixed 1:10 with CD45.1⁺ wildtype

Fig. 2 Oncogenic RAS confers increased progenitor numbers and self-renewal properties on Cux1^{low} HSPCs. **A** HSPC populations were quantified at 6–8 weeks post-treatment, before the development of disease. Absolute cell counts of LT-HSC (LSK⁺/CD34⁺/Flt3⁻), ST-HSC (LSK⁺/CD34⁺/Flt3⁻), and MPP (LSK⁺/CD34⁺/Flt3⁺) in the bone marrow are shown. For myeloid progenitor cells, absolute cell counts of CMP (Lin⁻/Kit⁺/Sca1⁻/CD34⁺/CD16/32^{low}), GMP (Lin⁻/Kit⁺/Sca1⁻/CD34⁺/CD16/32^{high}), and MEP (Lin⁻/Kit⁺/Sca1⁻/CD34⁺/CD16/32⁻) in the bone marrow were also quantified. Data represent mean of $n = 3–6$ per genotype \pm SEM. **B** Bone marrow cells isolated from mice treated for 6–8 weeks were tested in CFU assays containing doxycycline. Data represent one of three biological replicates. At each passage, cells were collected, and 25,000 cells were re-plated, with 7–11 days between each passage. CFU-GM were counted at the end of each passage. **C** Serial competitive bone marrow transplantation assays were performed in lethally irradiated CD45.1⁺ recipients with a 10:1 ratio of total bone marrow from CD45.1⁺ wildtype competitor cells and CD45.2⁺ experimental bone marrow as described in the Methods. At the end of the primary transplant, bone marrow cells were collected from two mice representing the median reconstitution and transplanted into secondary recipients ($n = 6–7$ recipients per experimental group). Data represent the total donor leukocyte (CD45⁺), B cell (B220⁺), and granulocyte (Gr1⁺/CD11b⁺) reconstitution at the indicated weeks. Data represent the mean \pm SD. For statistical comparisons: # = Ren;Nras^{WT} vs. Ren;Nras^{G12D}; * = Cux1^{low};Nras^{WT} vs. Cux1^{low};Nras^{G12D} or Ren;Nras^{WT}; \$ = Ren;Nras^{G12D} vs. Cux1^{low};Nras^{G12D}. **D** The absolute cell count of donor-derived LT-HSCs (CD45.2⁺/LSK⁺/CD150⁺/CD48⁺) and MPPs (CD45.2⁺/LSK⁺/CD150⁻/CD48⁻) were quantified at the end of each transplant. Each dot represents one biological replicate. Two-tailed Student *t* test was used to assess statistical significance. *, #, or \$ $p < 0.05$; **, ##, or \$\$ $p < 0.01$; and ***, ###, or \$\$\$ $p < 0.001$.

competitor bone marrow and transplanted to lethally irradiated CD45.1⁺ mice. The mice were monitored for 16 weeks, bone marrow was collected, and transplanted into new recipients, for a total of four serial transplants. Consistent with prior reports, Nras^{G12D} bone marrow had higher levels of reconstitution and self-renewal, up through the 4th transplant (Fig. 2C) [35]. Cux1^{low} bone marrow cells initially had increased competitiveness in myeloid lineages compared to Ren;Nras^{WT} controls, as we reported previously [19]. Nonetheless, this advantage extinguished in the quaternary transplant, consistent with HSC exhaustion (Fig. 2C). The addition of the Nras^{G12D} allele significantly mitigated this phenotype and enabled continued Cux1^{low} HSC self-renewal and multi-lineage production. Based on a limiting dilution analysis of Lin⁻/Sca1⁺/Kit⁺/CD150⁺/CD48⁻ cells, the combination of Nras^{G12D} and Cux1^{low} did not substantially increase the functional capacity of individual HSCs (Supplementary Fig. 3, Ren;Nras^{WT} vs. Cux1^{low};Nras^{G12D} $p = 0.066$). Rather, the combination of alleles increased the absolute numbers of LT-HSC and MPP, particularly in later transplants when control and Cux1^{low} counterparts are extremely diminished (Fig. 2D). Of note, MPPs containing Nras^{G12D} gain long-term multilineage reconstitution potential [35], consistent with the increase in Cux1^{low} MPPs observed with the addition of Nras^{G12D}. Thus, Nras^{G12D} imparts increased, long-term self-renewal on CUX1-deficient repopulating cells which would otherwise exhaust.

CUX1-knockdown enhances RAS signaling and cell cycling

A feature of JMML and CMML with RAS pathway mutations is hypersensitivity to growth factors and growth factor-independent colony formation [38, 39]. Given the CMML/JMML-like disease in some CUX1-knockdown;Nras^{G12D} mice, we tested the combined effect of Nras^{G12D} and CUX1-knockdown on growth factor responsiveness. To control for the finding that some experimental groups have increased numbers of progenitors (Fig. 2A), we plotted the results as absolute CFU numbers and normalized to the maximum number of CFUs, as performed previously [31, 39]. Compared to Ren;Nras^{WT} cells, Ren;Nras^{G12D} exhibited a greater number of CFUs, as reported (Fig. 3A and Supplementary Fig. 4) [31]. In response to IL3, the addition of CUX1-knockdown with Nras^{G12D} (Cux1^{low};Nras^{G12D}) led to a significant increase in CFUs compared to Nras^{G12D} alone (Fig. 3A, lower panel). In contrast, CUX1-knockdown in the absence of Nras^{G12D} did not alter cytokine responsiveness. For reasons that are unclear, CUX1-knockdown did not further increase the sensitivity of Nras^{G12D} bone marrow cells to GM-CSF (Supplementary Fig. 4). Discrepancies between IL3 and GM-CSF sensitivity have been observed previously [40].

We reasoned that increased IL3 sensitivity is accompanied by increased IL3 receptor signaling. To test this, we stimulated splenocytes from all six mouse genotypes with IL3 and measured

downstream signaling activity. By immunoblot, both Cux1^{mid} and Cux1^{low} alleles led to increased phosphorylation of ERK, AKT, and S6, downstream of IL3 receptor engagement (Fig. 3B and C). While Cux1^{low} alone modestly increased phospho-protein levels, the effect of Cux1^{mid} was most apparent in the context of Nras^{G12D}. We assessed if this elevated signaling is occurring in HSPCs (Lin⁻Kit⁺) via intracellular phospho-flow. CUX1-knockdown significantly increased p-ERK levels after either IL3 or SCF stimulation (Fig. 3D). Phospho-AKT was also highest in IL3-stimulated Cux1^{low};Nras^{G12D} HSPCs although this did not achieve statistical significance ($p = 0.15$). Overall, CUX1-knockdown increases signaling cascades downstream of growth factor receptors and RAS leading to increased growth factor sensitivity.

Compared to wildtype hematopoietic HSPCs, those with Nras^{G12D} or CUX1-knockdown have increased cell cycling [19, 35, 36, 41]. We next assessed if the combination of oncogenic RAS and loss of CUX1 further promotes cell cycling. HSPC populations were collected from mice six weeks post-transgene induction and assessed by intracellular flow. Compared to Cux1^{low} or Nras^{G12D} single mutant HSCs, Cux1^{low};Nras^{G12D} LT- and short-term- (ST-) HSCs were less quiescent (G_0) and more often in the G_1 cell cycle stage (Fig. 4). MPP, GMP, and megakaryocyte-erythroid progenitors (MEP) exhibited similar changes. Cux1^{low};Nras^{G12D} CMPs, and to a lesser extent, MPPs, were more often in S/G₂/M stages (Fig. 4). Overall, the addition of CUX1-knockdown and Nras^{G12D} increases the frequency of cycling stem and progenitor cells.

CUX1-knockdown and Nras^{G12D} have a convergent transcriptional program and down-regulate negative regulators of RAS/PI3K signaling

To assess a transcriptional role for CUX1 in regulating the RAS signaling pathway, we performed transcriptome analysis of HSCs (Lin⁻/Sca1⁺/Kit⁺/Flt3⁻) after CUX1 knockdown. Consistent with the cell cycle analysis in mouse HSCs (Fig. 4) and our prior analysis of human CD34⁺ HSPCs [19], CUX1-knockdown induced proliferative pathways with concomitant reduction in HSC quiescent genes (Fig. 5A). We also observed an induction of the MTORC gene signature, as we noted previously in human cells [19]. CUX1 is known to activate *Pik3ip1* expression, a negative regulator of PI3K [9, 19]. As such, CUX1-knockdown causes decreased PIK3IP1 levels and corresponding increased PI3K signaling. To assess negative regulators of PI3K and RAS more globally, we compiled a list of genes ($n = 79$, Supplementary Table 2) that negatively regulate RAS and/or PI3K. These genes are generally decreased in the CUX1-deficient state, as shown by Gene Set Enrichment Analysis (GSEA, Fig. 5B) [42]. Fourteen genes, including *Pik3ip1*, are significantly decreased after CUX1-knockdown (FDR < 0.05, Fig. 5C). These data indicate that CUX1 controls multiple negative regulators of RAS/PI3K.

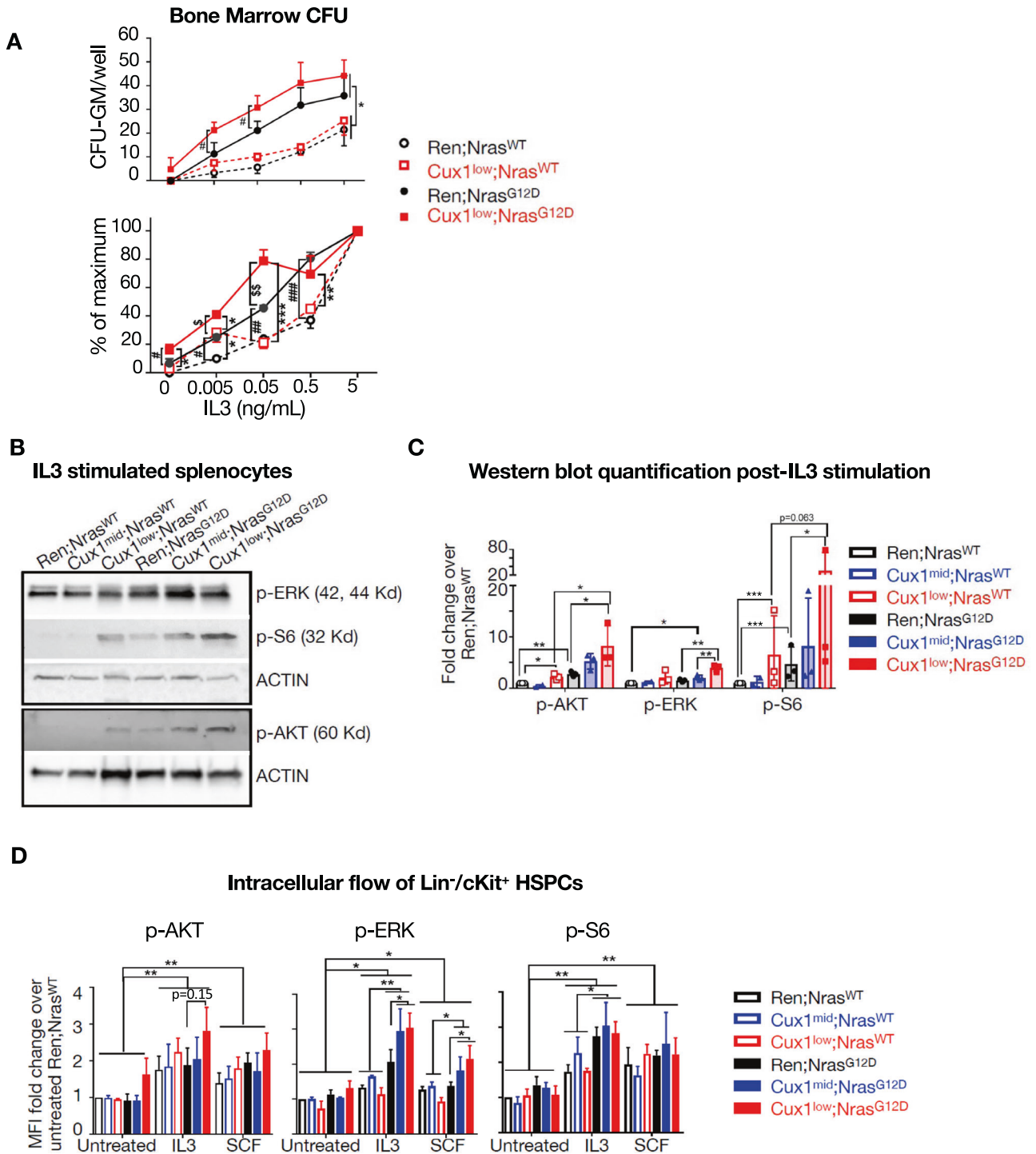


Fig. 3 CUX1 deficiency enhances RAS signaling. **A** Bone marrow cells were harvested from the indicated mouse genotypes after 6–8 weeks of doxycycline and poly I:C treatment and plated in methylcellulose. Myeloid colony numbers were enumerated in each condition. Percentage of maximum was calculated based on colony number in each condition relative to the colony number at the maximum concentration of IL3 (100%). Mean \pm SEM is shown for $n = 3$ biological replicates. * = $Cux1^{low};Nras^{WT}$ vs. $Cux1^{low};Nras^{G12D}$; # = $Ren;Nras^{WT}$ vs. $Ren;Nras^{G12D}$; § = $Ren;Nras^{G12D}$ vs. $Cux1^{low};Nras^{G12D}$. **B** Splenocytes collected from mice 6–8 weeks after poly I:C and doxycycline were stimulated with 100 ng/mL IL3 for 10 minutes and probed via immunoblot. **C** The level of p-ERK, p-S6, and p-AKT was quantified by measuring the pixel density of each protein using ImageJ densitometry software. Each dot represents one biological replicate. **D** Bone marrow cells collected from mice 6–8 weeks after poly I:C and doxycycline were analyzed by intracellular flow for p-ERK, p-S6, and p-AKT in Lin^{-}/Kit^{+} cells. Phospho-protein levels were quantified by median fluorescence intensity (MFI) and compared to $Ren;Nras^{WT}$ basal levels, which was assigned a value of 1. Data represent mean \pm SEM of $n = 3$ biological replicates. Two-tailed Student t test was used to assess statistical significance. *, #, or § $p < 0.05$; **, ##, or §§ $p < 0.01$; and ***, ###, or §§§ $p < 0.001$.

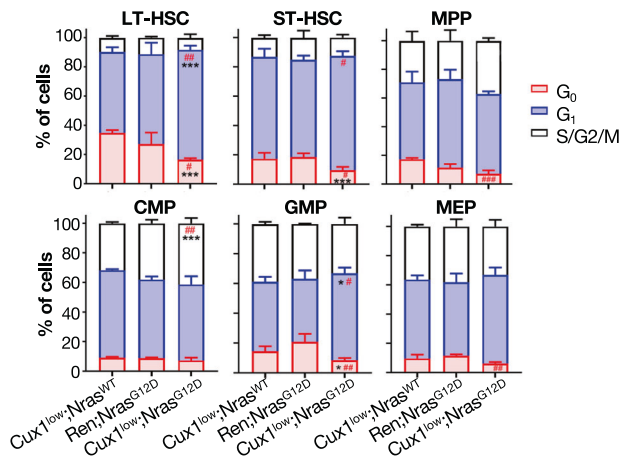


Fig. 4 The combination of CUX1 deficiency and Nras^{G12D} promotes HSPC cell cycling. Bone marrow cells were collected from Cux1^{low}; Nras^{WT}, Ren; Nras^{G12D} or Cux1^{low}; Nras^{G12D} mice 6 weeks after poly I:C and doxycycline treatment. Lin⁻ cells were isolated for intracellular flow analysis for Ki67 and DAPI and gated on the indicated HSPC populations. The bar graphs represent the mean \pm SD of $n = 3$ biological replicates. Two-tailed Student t test was used to assess statistical significance. * $p < 0.05$, ** $p < 0.01$, and *** $p < 0.001$ comparing Cux1^{low};Nras^{WT} vs. Cux1^{low};Nras^{G12D}. # $p < 0.05$, ## $p < 0.01$, and ### $p < 0.001$ comparing Cux1^{low};Nras^{G12D} vs. Ren;Nras^{G12D}.

To determine how CUX1-deficiency and oncogenic RAS interact at the transcriptomic level, we compared the Nras^{G12D} gene signature to that of CUX1. Specifically, we generated separate gene sets of transcripts downregulated or upregulated in Cux1^{low} cells. We then interrogated previously published RNA-seq data of Nras^{G12D} HSCs versus wildtype cells [43]. By GSEA, those genes downregulated in Cux1^{low} cells are also significantly decreased in Nras^{G12D} HSCs (NES = -1.190, $p = 0.032$, $q = 0.070$). Inversely, genes upregulated by CUX1-knockdown are also upregulated by Nras^{G12D} (NES = 1.421, $p = 0.008$, $q = 0.004$). This similarity is not explained solely by increased cell cycling; Nras^{G12D} did not significantly induce the proliferation (GSEA $p = 0.119$) nor reduce the quiescence gene signatures ($p = 0.328$). Overall, CUX1 deficiency and oncogenic NRAS impose overlapping gene signatures.

Taking this finding one step further, we asked what transcriptional impact Nras^{G12D} has on cells that are already deficient for CUX1. To test this, we generated RNA-seq data from Cux1^{low};Nras^{G12D} HSCs and compared it to Cux1^{low};Nras^{WT} cells. Even in a CUX1-deficient state, the addition of oncogenic NRAS further augments proliferative and CUX1 gene signatures (Fig. 5D) and reinforces the concept of overlapping transcriptional effects of the two mutations. Corresponding to the increase in proliferative transcripts, the addition of oncogenic NRAS also attenuated signatures of quiescent HSCs and LT-HSCs (Fig. 5D).

Overexpression of PIK3IP1 or SAMD9L inhibits the overgrowth of Cux1^{low};Nras^{G12D} HSPCs

While Nras^{G12D} alone did not associate with global changes in the negative regulators of RAS/PI3K (GSEA $p = 0.539$), expression of Nras^{G12D} in Cux1^{low} cells further decreased this gene set (Fig. 5E and Supplementary Fig. 5). Among down-regulated genes in the leading edge, *Samd9l* and *Pik3ip1* are the most highly expressed in HSCs (Fig. 5C and E). CUX1 directly binds 3 kb upstream of the *Pik3ip1* transcriptional start site and promotes *Pik3ip1* expression, an inhibitor of PI3K [9]. *Samd9l* also attracted our attention as inherited mutations in *SAMD9L* carry a risk of myeloid malignancies with monosomy 7 [44]. Moreover, *SAMD9L* has been described as a tumor suppressor that normally degrades cytokine

receptors—*SAMD9L* deficiency thereby sensitizes cells to growth factors [45]. For these reasons, we validated the decrease in *Pik3ip1* and *Samd9l* by quantitative RT-PCR (Fig. 6A) and by immunoblot (Fig. 6B and C) following loss of CUX1. The additional activation of NRAS in CUX1-knockdown cells further decreased expression of these genes. Hence, CUX1 deficiency, especially with the addition of oncogenic RAS, abates expression of multiple negative regulators of RAS/PI3K signaling, including *Pik3ip1* and *Samd9l*.

We tested whether restoration of *SAMD9L* or *PIK3IP1* would reverse the overgrowth of Cux1^{low};Nras^{G12D} HSPCs. To this end, we transfected Kit⁺ cells with *PIK3IP1* cDNA and performed CFU assays. Overexpression of *PIK3IP1* restored Cux1^{low};Nras^{G12D} CFU formation to numbers comparable to Ren control (Fig. 6D and E). Similarly, Cux1^{low};Nras^{G12D} Kit⁺ cells transduced with *SAMD9L* also had significantly reduced colony numbers compared to cells transduced with control virus (Fig. 6F and G). Overall, these data indicate that combined CUX1-deficiency and oncogenic NRAS lead to decreased expression of *PIK3IP1* and *SAMD9L*, and restoration of these proteins normalizes HSPC colony formation.

Decreased CUX1 levels augments sensitivity to PI3K and MEK inhibitors

Given the increased growth factor responsiveness and elevated signaling activity in Cux1^{low};Nras^{G12D} HSPCs, we predicted this characteristic would confer a therapeutic opportunity. For this reason, we tested the effects of PI3K or MEK inhibition on the growth of these cells. We selected pictilisib (GDC-0941), an orally available inhibitor of class I PI3K in clinical trials with preclinical activity in mouse models of RAS-driven MDS/MPN [46]. We also tested the FDA-approved drug, trametinib (GSK1120212), a potent, selective inhibitor of MEK1/2 that has shown efficacy in preclinical studies of Nras^{G12D}-driven myeloid neoplasms [47]. In CFU assays with increasing doses of either of these drugs, Ren;Nras^{G12D} bone marrow cells show a reduction of CFU formation. While Cux1^{low};Nras^{G12D} cells exhibit increased CFU formation in the absence of drugs, even low doses of either pictilisib or trametinib significantly abated CFU formation, to an extent similar to that of Ren;Nras^{G12D} cells (Fig. 7A). Thus, the growth advantage bestowed on Nras^{G12D} cells by CUX1-knockdown is dependent on PI3K and MEK signaling.

To determine if CUX1 levels correlate with MEK or PI3K inhibition in primary patient samples, we turned to the BEAT AML dataset, comprised of 326 patient samples tested *ex vivo* for sensitivity to 122 small-molecule inhibitors [48]. Across patient samples, we correlated each drug area-under-the-curve (AUC) to the expression level of CUX1. Of the 16 drugs classified as PI3K or MEK inhibitors, 12 had a significant positive correlation with CUX1 levels (FDR < 0.10, Fig. 7B, Supplementary Table 3). In other words, as CUX1 levels decrease, the AUC for these classes of drugs also decreased, indicating a greater sensitivity to the drug. Pictilisib and trametinib were among the significant correlations, with selumetinib (AZD6244), a MEK inhibitor, showing the strongest correlation. To exclude the possibility that this result is confounded by the presence RAS pathway mutations in AMLs with lower CUX1 levels, we repeated the analysis after removing samples with RAS pathway mutations. This second analysis corroborated the first (Fig. 7C). Accordingly, low levels of CUX1 correspond to increased sensitivity to PI3K and MEK inhibition in primary AML samples.

DISCUSSION

The connection between monosomy 7 and RAS mutations in myeloid malignancies stretches back over 30 years [49], yet the mutual affinity between these genetic events remained unexplained. Leveraging the power of consortia-driven cancer genomic datasets and mouse models, we explicitly link the chromosome 7

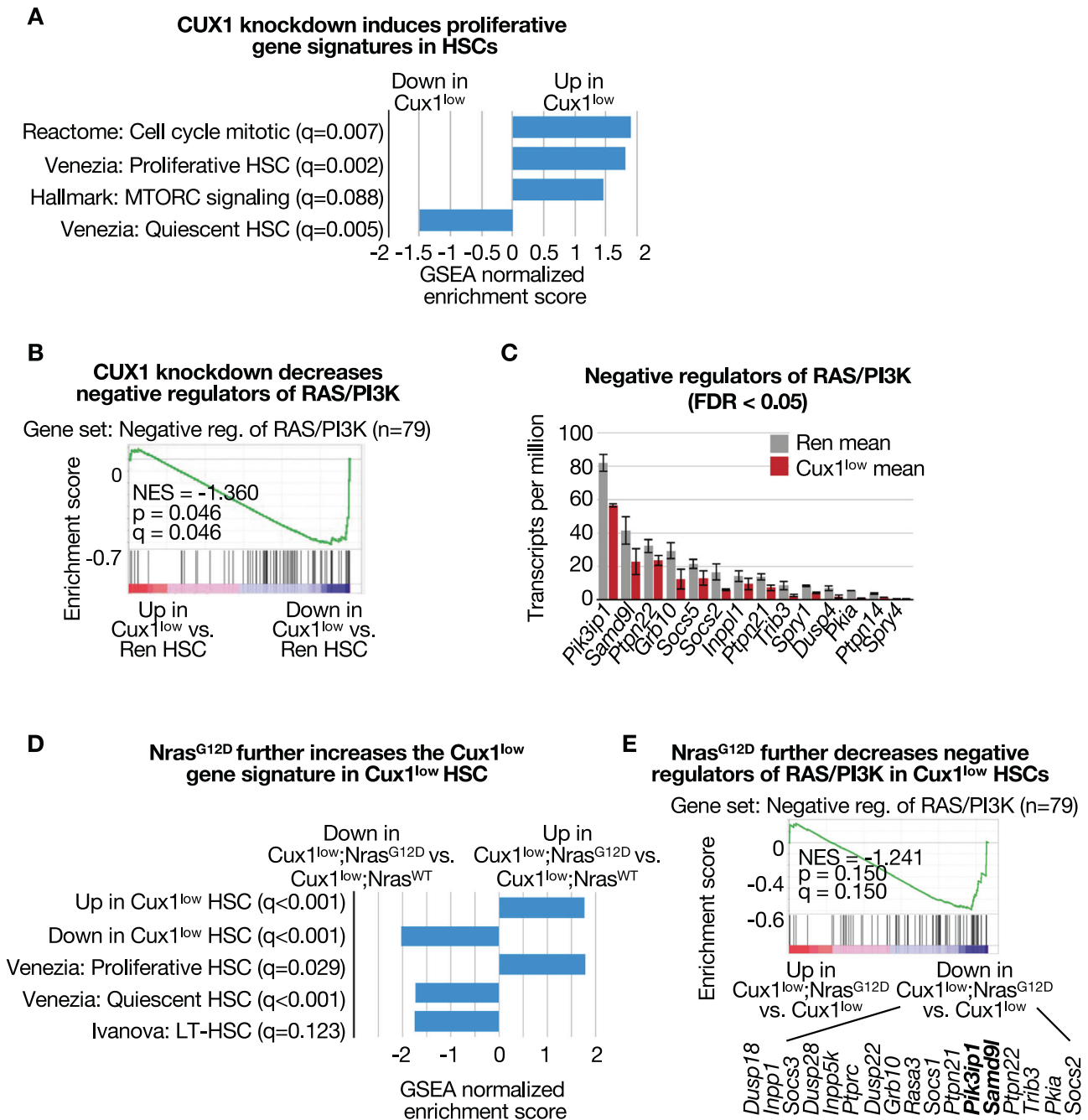


Fig. 5 **CUX1 knockdown and $Nras^{G12D}$ have a convergent transcriptional program and down-regulate negative regulators of RAS/PI3K signaling.** **A, B** GSEA of RNA-sequencing of HSCs ($LSK^+/Flt3^-$) from Ren and $Cux1^{low}$ mice treated for 5 days with doxycycline ($n = 3$ per genotype) [22]. **C** RNA-sequencing-derived levels of negative regulator of RAS/PI3K pathway genes with an FDR < 0.05. **D, E** GSEA of RNA-sequencing data comparing HSCs from $Cux1^{low};Nras^{WT}$ and $Cux1^{low};Nras^{G12D}$ mice. HSCs were collected 6 weeks post poly I:C and doxycycline treatment. In **E**, genes in the leading edge are listed.

encoded tumor suppressor gene, *CUX1*, with RAS mutations. Mechanistically, *CUX1* deficiency and oncogenic RAS promoted overlapping gene expression changes. RAS signaling can impact the transcriptome in multiple ways, including via the activation of AP-1 transcription factors [50]. The effects of RAS and *CUX1* were not redundant, as the addition of $Nras^{G12D}$ further augmented the *CUX1*-knockdown gene signature. *CUX1*-knockdown led to decreased expression of negative regulators of RAS/PI3K signaling, and $Nras^{G12D}$ magnified these changes. As a result, *CUX1*-knockdown; $Nras^{G12D}$ HSPCs had increased signaling downstream of growth factor receptors, resulting in heightened growth factor

sensitivity. Based on this, we propose a model wherein *CUX1* normally restrains the proliferative effects of growth factors via transcriptional regulation of negative regulators of signaling (Fig. 8A). With insufficient *CUX1*, decreased expression of *Pik3ip1*, *Samd9l*, and perhaps others, licenses unrestrained RAS signaling downstream of cytokine receptors (Fig. 8B). In agreement with this model, inhibitors of PI3K and MEK mitigate the effects of *CUX1* loss. The effectiveness of these drug classes also correlates with *CUX1* expression in AML patient samples. We posit that these inhibitors may have therapeutic value for patients with monosomy 7-associated myeloid malignancies. Additionally, RAS pathway

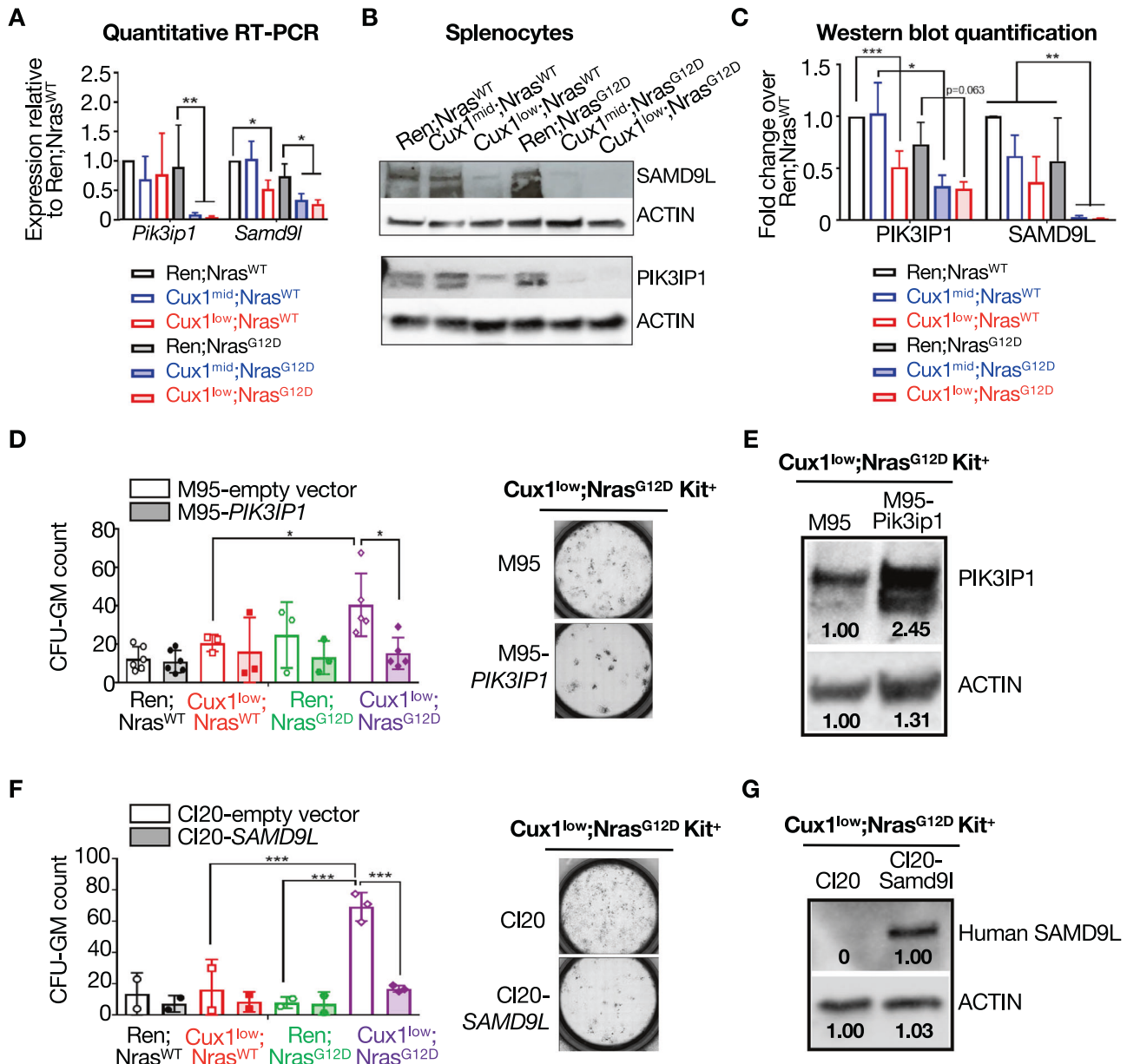


Fig. 6 Overexpression of PIK3IP1 or SAMD9L reduces Cux1^{low};Nras^{G12D} colony overgrowth. **A** Quantitative RT-PCR of the indicated genes from splenocytes collected from mice 5–7 weeks after poly I:C and doxycycline treatment. Mean \pm SEM is shown for $n = 3–7$ biological replicates per genotype. **B** Representative immunoblots of splenocytes for the indicated proteins. **C** Mean \pm SEM quantification is shown for immunoblots of $n = 4–6$ biological replicates per genotype. **D** Kit⁺ cells isolated from the indicated mice were transfected with *PIK3IP1* cDNA or empty-vector control plasmid and CFU assays were performed. CFU-GM colonies were enumerated on day 10 ($n = 3–6$ biological replicates per genotype). Representative CFU images are shown on the right. **E** Representative *PIK3IP1* immunoblot of cells collected after the CFU assay ($n = 3$). The pixel density is shown for individual bands quantified using ImageJ densitometry software. **F** Kit⁺ cells isolated from indicated mice were infected with *CI20-SAMD9L*-lentivirus or empty vector and assayed for CFU formation ($n = 2–3$ biological replicates per genotype). The CFU-GM colonies were enumerated on day 10. Representative CFU images are shown on the right. **G** Representative *SAMD9L* immunoblot of cells collected after the CFU assay ($n = 3$). The pixel density is shown for individual bands. Two-tailed Student *t* test was used to assess statistical significance. * $p < 0.05$, ** $p < 0.01$, and *** $p < 0.001$.

inhibitors may be beneficial for solid tumors with *CUX1* inactivating mutations; future studies in this vein are warranted.

The finding that *CUX1* loss and oncogenic RAS converge on a similar pathway is antithetical to two, albeit related, perennial axioms in cancer biology. First, is the exclusivity principle, wherein if the functional effect of two mutations is redundant, only one of these mutations is present in any single tumor, exhibiting negative genetic epistasis [51]. Elegant work by van de Haar, et al., has revealed the caveats with this assumption [52]. Second is the division of cancer drivers into separate, complementary

classes [28]. Class I pro-proliferation oncogenes are exemplified by kinases. Mutations in class II tumor suppressor genes impair differentiation and are represented by transcriptional regulators. In this paradigm, mutations in both classes cooperate in carcinogenesis. While *CUX1* is essential for differentiation [19], we also show herein that *CUX1* regulates oncogenic kinase cascades. Likewise, it is inarguable that aberrant RAS signaling disrupts differentiation [31, 53]. Our results blur the distinction between gross categorization of cancer drivers – their classification requires more nuance.

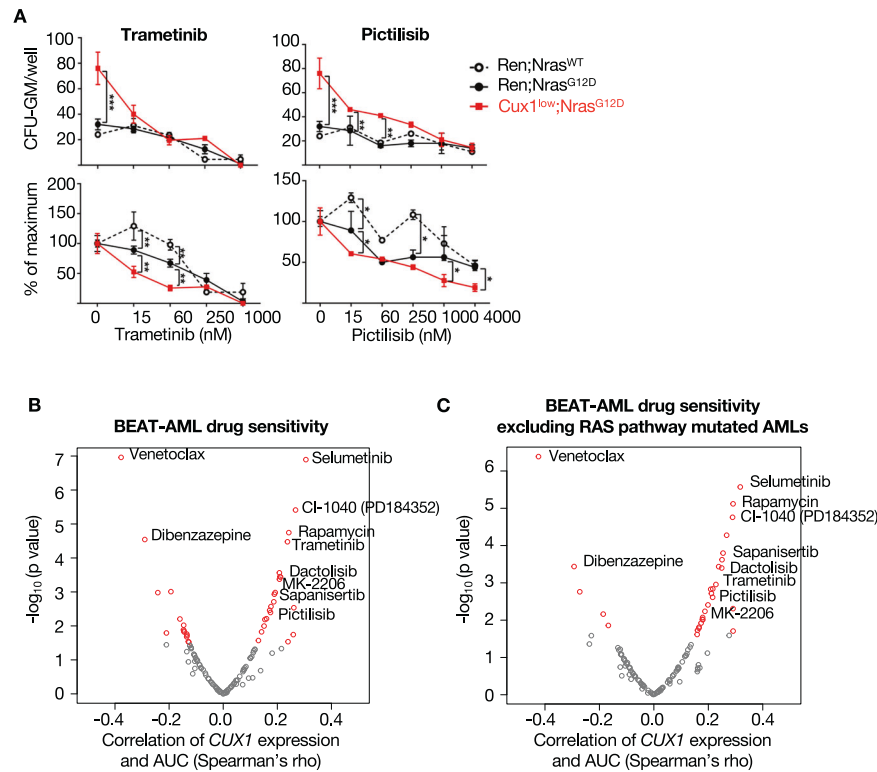


Fig. 7 Low levels of *CUX1* confer sensitivity to MEK and PIK3 inhibition in mouse HSPCs and human AMLs. **A** CFU assays were performed with bone marrow cells from mice collected 5–7 weeks post-treatment with poly I:C and doxycycline. Cells were cultured in 5 ng/mL IL3 and increasing doses of pictilisib or trametinib. Absolute colony numbers are indicated in the top panels. Bottom panels indicate the % of maximum CFU formation. One representative experiment of $n = 3$ is shown. Two-tailed Student t test was used to assess statistical significance. (* $p < 0.05$, ** $p < 0.01$, *** $p < 0.001$). **B** The area-under-the curve (AUC) of 122 small molecule inhibitors were correlated to the level of *CUX1* expression from 326 primary patients AML samples from the BEAT-AML study [48]. Red points indicate $FDR < 0.05$ calculated by Storey's q value. **C** The AUC of 122 small molecule inhibitors was correlated to the level of *CUX1* expression from 242 primary patients AML samples without oncogenic RAS pathway mutations.

Our findings that *CUX1* loss and RAS converge on increased signaling harmonize with other studies. Kevin Shannon's lab has reported that RAS mutant cancers upregulate the mutant RAS allele in multiple ways, through increased RNA expression, loss of the wildtype allele, or copy number neutral loss of heterozygosity [54, 55]. Others have reported that it is not unusual to have more than one oncogenic driver mutation in both alleles of the same gene, including RAS genes, within a tumor [56]. These studies, along with our results, suggest that, for RAS, "more is more." This may translate into increased dependence of these tumors on that very pathway [54].

CUX1 mutations and -7/del(7q) are generally considered early events in myeloid neoplasia [4, 5, 12]. This is congruent with reports of *CUX1* mutations and -7/del(7q) in clonal hematopoiesis, thought to be a precursor to malignancy [2, 3, 7, 10, 11]. RAS pathway mutations, on the other hand, occur infrequently in clonal hematopoiesis and are often late events in myeloid transformation [12, 57]. These data imply that *CUX1* loss normally precedes RAS mutations. Among disease types, *CUX1* mutations are more often associated with MDS [9], fitting the disease phenotype we observed in *CUX1*-knockdown mice [19] (Fig. 8C). Oncogenic RAS mutations are associated with the transformation of MDS to AML [58], which is accurately modeled by the leukemic phenotype of *Cux1*^{low};*Nras*^{G12D} mice (Fig. 8D). Our results show that the transformative properties of RAS include not only enhancing oncogenic signaling but also increasing self-renewal of *CUX1*-deficient HSPCs.

The exception to this sequence of events is, of course, in the setting of inherited RASopathy gene mutations, where, by definition, the RAS pathway mutation is antecedent to loss of

chromosome 7 and *CUX1*. JMML infrequently transforms to AML, and case studies have shown that this transformation is associated with duplication of mutant RAS genes from acquired uniparental disomy [59]. This finding is concordant with the "more is more" model for RAS dosage in leukemic transformation. It is unknown if the order of *CUX1* loss and RAS influences the disease phenotype. One could surmise that antecedent *CUX1* loss associates with MDS, and a subsequent RAS mutation leads to secondary AML. When RAS mutations are first, then MDS/MPN such as JMML arise. Aly et al. did not find an association between the timing of *CUX1* loss and disease phenotype, however, the presence of RAS mutations was not included in their analysis [33]. Other variables may also confound this type of comparison. For instance, unlike MDS, JMML has a paucity of additional mutations that may influence the disease phenotype [25]. Further, the developmental timing of the RAS mutation may impact the disease manifestation [60].

In conclusion, our work demonstrates positive genetic epistasis between *CUX1* loss and oncogenic RAS in neoplasia. *CUX1* deficiency and activated RAS drive complementary and partially overlapping, but non-redundant transcriptional and cellular pathways to enforce HSPC signaling, proliferation, defective differentiation, and transformation.

METHODS

Mouse models

All animal studies were approved by The University of Chicago Institutional Animal Care and Use Committee. Mice were housed in Association for Assessment and Accreditation of Laboratory Animal Care-accredited, specific pathogen-free animal care facilities. Both sexes of mice were included. Ren,

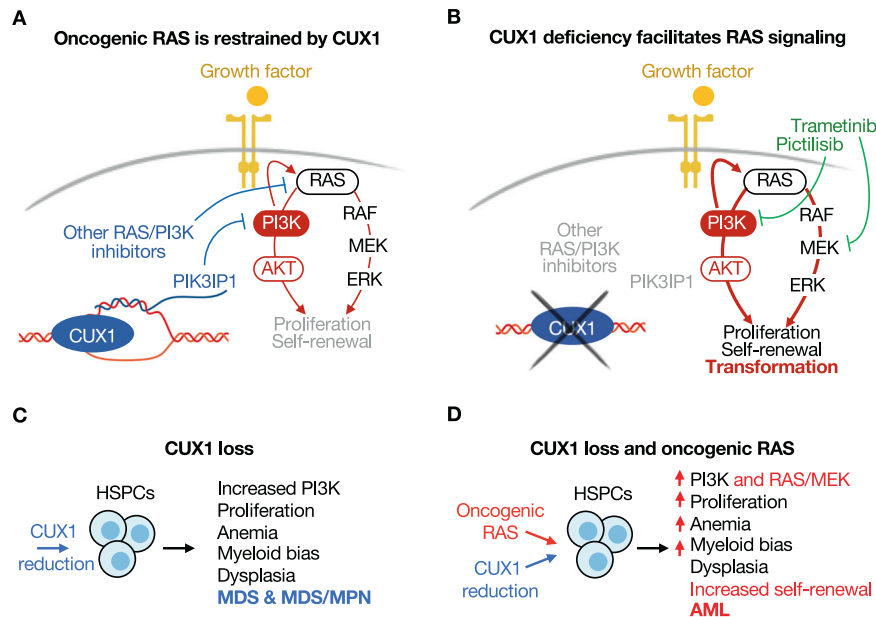


Fig. 8 Model for how CUX1 deficiency cooperates with activated RAS to promote leukemogenesis. **A** We propose a model wherein CUX1 normally transcriptionally activates expression of *PIK3IP1* and other RAS/PI3K inhibitors, thereby restraining RAS signaling. **B** CUX1 deficiency causes decreased expression of these regulators, resulting in increased PI3K and MEK mediated signaling and downstream proliferation and survival, accelerating transformation and promoting leukemogenesis. This aberrant signaling is responsive to PI3K or MEK blockade. **C** CUX1 deficiency alone drives several features of MDS, including anemia, myeloid bias, and multi-lineage dysplasia. **D** Oncogenic RAS exacerbates these defects further and additionally promotes HSPC self-renewal and overt AML transformation. Figures created in part using BioRender.com.

Cux1^{mid}, and *Cux1*^{low} mice were generated as previously described [19]. *Mx1-Cre*;*Nras*^{G12D} mice were generously provided by Dr. Kevin Shannon (University of California San Francisco). The breeding scheme to generate littermate controls is as follows. *Cux1*^{mid/ren};*M2rtTA*^{+/+} or *Cux1*^{low/ren};*M2rtTA*^{+/+} were crossed with *M2rtTA*^{+/+};*Mx1-Cre*^{+/+};*Nras*^{G12D/+} to generate *Cux1*^{mid/+};*M2rtTA*^{+/+};*Mx1-Cre*^{+/+};*Nras*^{G12D/+} (*Cux1*^{mid};*Nras*^{G12D}), *Cux1*^{low/+};*M2rtTA*^{+/+};*Mx1-Cre*^{+/+};*Nras*^{G12D/+} (*Cux1*^{low};*Nras*^{G12D}), *Cux1*^{ren/+};*M2rtTA*^{+/+};*Mx1-Cre*^{+/+};*Nras*^{G12D/+} (*Ren*;*Nras*^{G12D}). Mice generated by this scheme without *Mx1-Cre* were sometimes used as single mutation controls (*Ren*, *Cux1*^{mid}, and *Cux1*^{low}). Mice are on a C57BL/6 × 129/Sv background.

For all experiments, mice were 4 weeks and older. The shRNA transgene was induced by maintaining the mice on continuous doxycycline-containing chow diet (TD.120658, 1000 mg/kg, Envigo). To induce *Mx1-Cre* expression, mice were injected intraperitoneally with 10 mg/kg of poly I:C (Sigma Aldrich) every other day for three doses. Mouse genotyping was performed by Transnetyx, Inc.

Histology

Tissues were prepared as previously described [22]. Anti-GATA1 (D52H6) was from Cell Signaling Technologies.

Colony forming unit (CFU) assays

50,000 bone marrow cells from mice treated with poly I:C and doxycycline for 4–6 weeks were assessed as described [19]. For cytokine sensitivity assay, 30,000 bone marrow cells were cultured in 1 µg/mL doxycycline-containing methylcellulose (MethoCult M3231) with recombinant murine GM-CSF or IL3 (PeproTech). For inhibitor studies, the methylcellulose was supplemented with 5 ng/mL of IL3 and pictilisib (GDC-0941, Genentech) or trametinib (GSK1120212, Selleckchem). For CFUs with *Kit*⁺ cells, 1000–3000 *Kit*⁺ cells were plated after transfection or transduction.

Western blot

Red blood cell lysed splenocytes were collected 6–8 weeks post doxycycline and poly I:C treatment. Cells were starved in RPMI with 0.1% FBS low serum for 2 hours, then stimulated with or without 100 ng/mL IL3 (PeproTech) for 10 minutes. Stimulation was stopped by 10-fold dilution in cold PBS. The lysates were probed as described [19] with p-AKT (S473, 193H12, Cell Signaling), p-ERK (p44/42, 137F5, Cell Signaling), or p-S6

(S240/244, Cell Signaling). Unstimulated cells were probed for *PIK3IP1* (16826-1, Protein Technology), *SAMD9L* (PA5-25090, Thermo Fisher), and β -ACTIN (C4, SC-47778, Santa Cruz). Immunoblots were quantified using ImageJ.

RNA-seq

Two RNA-seq experiments were performed. The first compared *Cux1*^{low/+};*M2rtTA*^{+/+} to *Ren*;*M2rtTA*^{+/+} hematopoietic stem cells (HSC) sorted from the bone marrow of mice after five days of doxycycline, with three biological replicates (GEO accession GSE154674) [22]. The second compared *Cux1*^{low};*Nras*^{WT} ($n=2$) with *Cux1*^{low};*Nras*^{G12D} ($n=3$) (GEO accession GSE161614, Supplementary Table 1). *Lin*⁻/*Kit*⁺/*Sca1*⁺/*CD135*⁻ HSCs were flow sorted 5 weeks post poly I:C and doxycycline treatment. RNA-seq libraries were generated and analyzed as previously [22]. For gene set enrichment analysis, “Quiescent” and “Proliferative” gene sets were obtained from ref. [61]. The “Negative regulators of RAS/PI3K” was generated by literature and gene ontology review (Supplementary Table 2).

Quantitative RT-PCR

RNA was quantified as described [19] with the following primers:

Mouse- <i>Pik3ip1</i> -F	CCATGGAGCTGGAAGAGAAG
Mouse- <i>Pik3ip1</i> -R	AGCTCCAATAGCGAGGATGA
Mouse- <i>Gapdh</i> -F	GTGGAGTCATACTGGAACATGTAG
Mouse- <i>Gapdh</i> -R	AATGGTGAAGGTCGGTGTG
Mouse- <i>Samd9L</i> -F	CCTGGTGTCTCTCAGCCAGT
Mouse- <i>Samd9L</i> -R	CTTCATTCTGCCCTGTCTCC

Transfection

Human *PIK3IP1* (NM_052880.4, EX-11822-M95, Genecopoeia) was over-expressed in the mCherry⁺ pReceiver-M95 plasmid. Empty vector (pEX-

NEG-M95) was used as a control. 5×10^5 freshly isolated or recovered cryopreserved mouse bone marrow Kit⁺ cells were electroporated with 1 µg of plasmid using Neon (Thermo Fisher) at 1900 V, 20 ms, 1 pulse.

Lentivirus generation and transduction

Lentivirus was generated by transfecting the lentiviral DNA and packaging plasmids into HEK293T cells using Lipofectamine 2000 (Thermo Fisher) at a 7:4:3 ratio of lentiviral vector:drR8.74:pMD2 VSVG. The pCL20c-MSCV-IRES-mCherry (nFlag-human-SAMD9L) and pCL20c-MSCV-IRES-mCherry (control) plasmids were generously provided by Dr. Jeffrey Klco [62]. Transduction was performed as described [6]. mCherry⁺ Kit⁺ cells were flow sorted 2 days post-transduction.

Complete methods are provided in the Supplementary Methods.

DATA AVAILABILITY

The datasets generated during the current study are available in the GEO repository, accession [GSE161614](https://www.ncbi.nlm.nih.gov/geo/query/acc.cgi?acc=GSE161614).

REFERENCES

- Jotte MRM, McNerney ME. The significance of CUX1 and chromosome 7 in myeloid malignancies. *Curr Opin Hematol*. 2022;29:92–102.
- Laurie CC, Laurie CA, Rice K, Doheny KF, Zelnick LR, McHugh CP, et al. Detectable clonal mosaicism from birth to old age and its relationship to cancer. *Nat Genet*. 2012;44:642–50.
- Loh PR, Genovese G, Handsaker RE, Finucane HK, Reshef YA, Palamara PF, et al. Insights into clonal haematopoiesis from 8,342 mosaic chromosomal alterations. *Nature*. 2018;559:350–5.
- Dimitriou M, Woll PS, Mortera-Blanco T, Karimi M, Wedge DC, Doolittle H, et al. Perturbed hematopoietic stem and progenitor cell hierarchy in myelodysplastic syndromes patients with monosomy 7 as the sole cytogenetic abnormality. *Oncotarget*. 2016;7:72685–98.
- Takahashi K, Wang F, Kantarjian H, Song X, Patel K, Neelapu S, et al. Copy number alterations detected as clonal hematopoiesis of indeterminate potential. *Blood Adv*. 2017;1:1031–6.
- McNerney ME, Brown CD, Wang X, Bartom ET, Karmakar S, Bandlamudi C, et al. CUX1 is a haploinsufficient tumor suppressor gene on chromosome 7 frequently inactivated in acute myeloid leukemia. *Blood*. 2013;121:975–83.
- Jaiswal S, Fontanillas P, Flannick J, Manning A, Grauman PV, Mar BG, et al. Age-related clonal hematopoiesis associated with adverse outcomes. *N Engl J Med*. 2014;371:2488–98.
- Lindsley RC, Saber W, Mar BG, Redd R, Wang T, Haagenson MD, et al. Prognostic mutations in myelodysplastic syndrome after stem-cell transplantation. *N Engl J Med*. 2017;376:536–47.
- Wong CC, Martincorena I, Rust AG, Rashid M, Alifrangis C, Alexandrov LB, et al. Inactivating CUX1 mutations promote tumorigenesis. *Nat Genet*. 2014;46:33–8.
- Gibson CJ, Lindsley RC, Tchekmedyian V, Mar BG, Shi J, Jaiswal S, et al. Clonal hematopoiesis associated with adverse outcomes after autologous stem-cell transplantation for lymphoma. *J Clin Oncol*. 2017;35:1598–605.
- Zink F, Stacey SN, Norddahl GL, Frigge ML, Magnusson OT, Jonsdottir I, et al. Clonal hematopoiesis, with and without candidate driver mutations, is common in the elderly. *Blood*. 2017;130:742–52.
- Papaemmanuil E, Gerstung M, Malcovati L, Tauro S, Gundem G, Van Loo P, et al. Clinical and biological implications of driver mutations in myelodysplastic syndromes. *Blood*. 2013;122:3616–27.
- Ludlow C, Choy R, Blochlinger K. Functional analysis of Drosophila and mammalian cut proteins in flies. *Dev Biol*. 1996;178:149–59.
- Sinclair AM, Lee JA, Goldstein A, Xing D, Liu S, Ju R, et al. Lymphoid apoptosis and myeloid hyperplasia in CCAAT displacement protein mutant mice. *Blood*. 2001;98:3658–67.
- Sansregret L, Nepveu A. The multiple roles of CUX1: insights from mouse models and cell-based assays. *Gene*. 2008;412:84–94.
- Alcalay NI, Sharma M, Vassmer D, Chapman B, Paul B, Zhou J, et al. Acceleration of polycystic kidney disease progression in cpk mice carrying a deletion in the homeodomain protein Cux1. *Am J Physiol Ren Physiol*. 2008;295:F1725–34.
- Cubelos B, Sebastian-Serrano A, Beccari L, Calcagnotto ME, Cisneros E, Kim S, et al. Cux1 and Cux2 regulate dendritic branching, spine morphology, and synapses of the upper layer neurons of the cortex. *Neuron*. 2010;66:523–35.
- Lizarraga G, Lichtler A, Upholt WB, Kosher RA. Studies on the role of Cux1 in regulation of the onset of joint formation in the developing limb. *Dev Biol*. 2002;243:44–54.
- An N, Khan S, Imgruet M, Gurbuxani SK, Konecki SN, Burgess M, et al. Gene dosage effect of CUX1 in a murine model disrupts HSC homeostasis and controls the severity and mortality of MDS. *Blood*. 2018;131:2682–97.
- Arthur RK, An N, Khan S, McNerney ME. The haploinsufficient tumor suppressor, CUX1, acts as an analog transcriptional regulator that controls target genes through distal enhancers that loop to target promoters. *Nucleic Acids Res*. 2017;45:6350–61.
- Ramdzan ZM, Nepveu A. CUX1, a haploinsufficient tumour suppressor gene overexpressed in advanced cancers. *Nat Rev Cancer*. 2014;14:673–82.
- Imgruet MK, Lutze J, An N, Hu B, Khan S, Kurkewich J, et al. Loss of a 7q gene, CUX1, disrupts epigenetic-driven DNA repair and causes therapy-related myeloid neoplasms. *Blood*. 2021;138:790–805.
- Luna-Fineman S, Shannon KM, Lange BJ. Childhood monosomy 7: epidemiology, biology, and mechanistic implications. *Blood*. 1995;85:1985–99.
- Side LE, Curtiss NP, Teel K, Kratz C, Wang PW, Larson RA, et al. RAS, FLT3, and TP53 mutations in therapy-related myeloid malignancies with abnormalities of chromosomes 5 and 7. *Genes Chromosomes Cancer*. 2004;39:217–23.
- Stieglitz E, Taylor-Weiner AN, Chang TY, Gelston LC, Wang YD, Mazor T, et al. The genomic landscape of juvenile myelomonocytic leukemia. *Nat Genet*. 2015;47:1326–33.
- Luna-Fineman S, Shannon KM, Atwater SK, Davis J, Masterson M, Ortega J, et al. Myelodysplastic and myeloproliferative disorders of childhood: a study of 167 patients. *Blood*. 1999;93:459–66.
- McNerney ME, Brown CD, Peterson AL, Banerjee M, Larson RA, Anastasi J, et al. The spectrum of somatic mutations in high-risk acute myeloid leukaemia with -7/del(7q). *Br J Haematol*. 2014;166:550–6.
- Kelly LM, Gilliland DG. Genetics of myeloid leukemias. *Annu Rev Genom Hum Genet*. 2002;3:179–98.
- Chang TY, Dvorak CC, Loh ML. Bedside to bench in juvenile myelomonocytic leukemia: insights into leukemogenesis from a rare pediatric leukemia. *Blood*. 2014;124:2487–97.
- Bacher U, Haferlach T, Schoch C, Kern W, Schnittger S. Implications of NRAS mutations in AML: a study of 2502 patients. *Blood*. 2006;107:3847–53.
- Li Q, Haigis KM, McDaniel A, Harding-Theobald E, Kogan SC, Akagi K, et al. Hematopoiesis and leukemogenesis in mice expressing oncogenic NrasG12D from the endogenous locus. *Blood*. 2011;117:2022–32.
- Haigis KM, Kendall KR, Wang Y, Cheung A, Haigis MC, Glickman JN, et al. Differential effects of oncogenic K-Ras and N-Ras on proliferation, differentiation and tumor progression in the colon. *Nat Genet*. 2008;40:600–8.
- Aly M, Ramdzan ZM, Nagata Y, Balasubramanian SK, Hosono N, Makishima H, et al. Distinct clinical and biological implications of CUX1 in myeloid neoplasms. *Blood Adv*. 2019;3:2164–78.
- Kogan SC, Ward JM, Anver MR, Berman JJ, Brayton C, Cardiff RD, et al. Bethesda proposals for classification of nonlymphoid hematopoietic neoplasms in mice. *Blood*. 2002;100:238–45.
- Li Q, Bohin N, Wen T, Ng V, Magee J, Chen SC, et al. Oncogenic Nras has bimodal effects on stem cells that sustainably increase competitiveness. *Nature*. 2013;504:143–7.
- Wang J, Kong G, Liu Y, Du J, Chang Yi, Tey SR, et al. Nras(G12D/+) promotes leukemogenesis by aberrantly regulating hematopoietic stem cell functions. *Blood*. 2013;121:5203–7.
- Dovey OM, Cooper JL, Mupo A, Grove CS, Lynn C, Conte N, et al. Molecular synergy underlies the co-occurrence patterns and phenotype of NPM1-mutant acute myeloid leukemia. *Blood*. 2017;130:1911–22.
- Geissler K, Hinterberger W, Bettelheim P, Haas O, Lechner K. Colony growth characteristics in chronic myelomonocytic leukemia. *Leuk Res*. 1988;12:373–7.
- Emanuel PD, Bates LJ, Castleberry RP, Gualtieri RJ, Zuckerman KS. Selective hypersensitivity to granulocyte-macrophage colony-stimulating factor by juvenile chronic myeloid leukemia hematopoietic progenitors. *Blood*. 1991;77:925–9.
- Kunimoto H, Meydan C, Nazir A, Whitfield J, Shank K, Rapaport F, et al. Cooperative epigenetic remodeling by TET2 loss and NRAS mutation drives myeloid transformation and MEK inhibitor sensitivity. *Cancer Cell*. 2018;33:44–59.e48.
- Wang J, Liu Y, Li Z, Wang Z, Tan LX, Ryu MJ, et al. Endogenous oncogenic Nras mutation initiates hematopoietic malignancies in a dose- and cell type-dependent manner. *Blood*. 2011;118:368–79.
- Subramanian A, Tamayo P, Mootha VK, Mukherjee S, Ebert BL, Gillette MA, et al. Gene set enrichment analysis: a knowledge-based approach for interpreting genome-wide expression profiles. *Proc Natl Acad Sci USA*. 2005;102:15545–50.
- Jin X, Qin T, Zhao M, Bailey N, Liu L, Yang K, et al. Oncogenic N-Ras and Tet2 haploinsufficiency collaborate to dysregulate hematopoietic stem and progenitor cells. *Blood Adv*. 2018;2:1259–71.
- Wong JC, Bryant V, Lamprecht T, Ma J, Walsh M, Schwartz J, et al. Germline SAMD9 and SAMD9L mutations are associated with extensive genetic evolution and diverse hematologic outcomes. *JCI Insight*. 2018;3:121086.

45. Nagamachi A, Matsui H, Asou H, Ozaki Y, Aki D, Kanai A, et al. Haploinsufficiency of SAMD9L, an endosome fusion facilitator, causes myeloid malignancies in mice mimicking human diseases with monosomy 7. *Cancer Cell*. 2013;24:305–17.
46. Akutagawa J, Huang TQ, Epstein I, Chang T, Quirindongo-Crespo M, Cottonham CL, et al. Targeting the PI3K/Akt pathway in murine MDS/MPN driven by hyperactive Ras. *Leukemia*. 2016;30:1335–43.
47. Burgess MR, Hwang E, Firestone AJ, Huang T, Xu J, Zuber J, et al. Preclinical efficacy of MEK inhibition in Nras-mutant AML. *Blood*. 2014;124:3947–55.
48. Tyner JW, Tognon CE, Bottomly D, Wilmot B, Kurtz SE, Savage SL, et al. Functional genomic landscape of acute myeloid leukaemia. *Nature*. 2018;562:526–31.
49. Shannon KM, Watterson J, Johnson P, O'Connell P, Lange B, Shah N, et al. Monosomy 7 myeloproliferative disease in children with neurofibromatosis, type 1: epidemiology and molecular analysis. *Blood*. 1992;79:1311–8.
50. Lavoie H, Gagnon J, Therrien M. ERK signalling: a master regulator of cell behaviour, life and fate. *Nat Rev Mol Cell Biol*. 2020;21:607–32.
51. Vogelstein B, Kinzler KW. Cancer genes and the pathways they control. *Nat Med*. 2004;10:789–99.
52. van de Haar J, Canisius S, Yu MK, Voest EE, Wessels LFA, Ideker T. Identifying epistasis in cancer genomes: a delicate affair. *Cell*. 2019;177:1375–83.
53. Wang T, Li C, Xia C, Dong Y, Yang D, Geng Y, et al. Oncogenic NRAS hyper-activates multiple pathways in human cord blood stem/progenitor cells and promotes myelomonocytic proliferation in vivo. *Am J Transl Res*. 2015;7:1963–73.
54. Xu J, Haigis KM, Firestone AJ, McNerney ME, Li Q, Davis E, et al. Dominant role of oncogene dosage and absence of tumor suppressor activity in Nras-driven hematopoietic transformation. *Cancer Discov*. 2013;3:993–1001.
55. Burgess MR, Hwang E, Mroue R, Bielski CM, Wandler AM, Huang BJ, et al. KRAS allelic imbalance enhances fitness and modulates MAP kinase dependence in cancer. *Cell*. 2017;168:817–29.e815.
56. Saito Y, Koya J, Araki M, Kogure Y, Shingaki S, Tabata M, et al. Landscape and function of multiple mutations within individual oncogenes. *Nature*. 2020;582:95–9.
57. Corces-Zimmerman MR, Hong WJ, Weissman IL, Medeiros BC, Majeti R. Pre-leukemic mutations in human acute myeloid leukemia affect epigenetic regulators and persist in remission. *Proc Natl Acad Sci USA*. 2014;111:2548–53.
58. Takahashi K, Jabbour E, Wang X, Luthra R, Bueso-Ramos C, Patel K, et al. Dynamic acquisition of FLT3 or RAS alterations drive a subset of patients with lower risk MDS to secondary AML. *Leukemia*. 2013;27:2081–3.
59. Niemeyer CM. JMML genomics and decisions. *Hematol Am Soc Hematol Educ Program*. 2018;2018:307–12.
60. Liu YL, Yan Y, Webster C, Shao L, Lensing SY, Ni H, et al. Timing of the loss of Pten protein determines disease severity in a mouse model of myeloid malignancy. *Blood*. 2016;127:1912–22.
61. Venezia TA, Merchant AA, Ramos CA, Whitehouse NL, Young AS, Shaw CA, et al. Molecular signatures of proliferation and quiescence in hematopoietic stem cells. *PLoS Biol*. 2004;2:e301.
62. Thomas ME, 3rd, Abdelhamed S, Hiltenbrand R, Schwartz JR, Sakurada SM, Walsh M, et al. Pediatric MDS and bone marrow failure-associated germline mutations in SAMD9 and SAMD9L impair multiple pathways in primary hematopoietic cells. *Leukemia*. 2021;35:3232–44.
63. Chakravarty D, Gao J, Phillips SM, Kundra R, Zhang H, Wang J, et al. OncoKB: a precision oncology knowledge base. *JCO Precis Oncol*. 2017;2017:PO.17.00011.

ACKNOWLEDGEMENTS

The authors are grateful for the services and assistance provided by the following University of Chicago core facilities supported by the Cancer Center Support Grant (P30 CA014599): Integrated Light Microscopy Core, Cytometry and Antibody Technology Core (RRID: SCR_017760), Human Tissue Resource Center (RRID: SCR_019199), and the Genomics Facility (RRID: SCR_019196). We also thank The University of Chicago's Center for Research Informatics Bioinformatics Core and Animal Resources Center. We thank Dr. Jeffrey Klco (St. Jude Children's Research Hospital) for providing the lentiviral plasmids. We also gratefully acknowledge Dr. Angela Stoddart for critical reading of the manuscript. The authors would like to acknowledge the American Association for Cancer Research and its financial and material support in the development of the AACR Project GENIE registry, as well as members of the consortium for their commitment to data sharing. Interpretations are the responsibility of the study authors.

This work was supported in part by the American Cancer Society Research Scholar Grant 132457-RSG-18-171-01-LIB, American Society of Hematology Junior Faculty Scholar Award, the National Institutes of Health (R01 HL142782 and R01 CA231880), the Brinson Foundation, and The University of Chicago Cancer Research Foundation Women's Board. MKI is supported by NIH F30 CA232673 and The University of Chicago Medical Scientist Training Program (T32 GM007281). The authors gratefully acknowledge the support of Robin and Matthew Patinkin.

AUTHOR CONTRIBUTIONS

NA and MEM conceived the experiments and wrote the manuscript. NA performed the mouse experiments and in vitro assays and analyzed data. SK assisted with mouse experiments and in vitro assays. NA and MKI performed RNA sequencing. MEM and MKI analyzed the RNA-seq data. MEM and LJ analyzed TCGA and GENIE data. SG performed hematopathologic analyses and edited the manuscript.

COMPETING INTERESTS

The authors declare no competing interests.

ADDITIONAL INFORMATION

Supplementary information The online version contains supplementary material available at <https://doi.org/10.1038/s41388-023-02612-x>.

Correspondence and requests for materials should be addressed to Megan E. McNerney.

Reprints and permission information is available at <http://www.nature.com/reprints>

Publisher's note Springer Nature remains neutral with regard to jurisdictional claims in published maps and institutional affiliations.

Springer Nature or its licensor (e.g. a society or other partner) holds exclusive rights to this article under a publishing agreement with the author(s) or other rightsholder(s); author self-archiving of the accepted manuscript version of this article is solely governed by the terms of such publishing agreement and applicable law.